

RESEARCH

Open Access



Design and analysis antennas of transverse polarization on the dielectric waveguide

Mohamed N. Shaaban^{1*} , Aydar R. Nasybullin^{2†} and Yuri E. Sedelnikov^{2†}

[†]These authors contributed equally to this work.

*Correspondence: eng.m.nor@azhar.edu.eg

¹ Electrical Engineering Department, Faculty of Engineering, Al Azhar University, Qena 83513, Egypt
² Institute of Radio Electronics, Photonics and Digital Technologies, Kazan National Research Technical University named after A.N. Tupolev-KAI, Kazan, Russia

Abstract

This paper addresses the issue of constructing millimeter band antennas using dielectric waveguide structures. A new type of linear antenna, incorporating metal pins on the side walls of the grooved dielectric waveguide, is proposed for generating polarization perpendicular to the waveguide axis. However, these antennas suffer from the drawback of cross-polarized radiation in directions close to the waveguide axis. To overcome this limitation, a modified antenna design with transverse polarization is introduced, featuring a closed groove waveguide with a longitudinal slot at the top of the wall. The paper provides a comparison between two types of dielectric waveguide antennas: first, waveguide antenna with grooves in the dielectric which results in longitudinal polarization, and second, waveguide antenna with quarter-wavelength pins which results in transverse polarization. Electrodynamic modeling data are provided to demonstrate the effectiveness of the proposed antennas for satellite, 5G antenna, and radar applications. Finally, an antenna of quarter-wavelength pins is proposed with a frequency of 39 GHz, a gain of 19.8 dBi, and a width of the radiation pattern of 3.2°, and a sidelobe level (SLL) of -13.3 dB has been achieved.

Keywords: Dielectric waveguides, Leaky-wave antennas, Periodic structures, Grooved dielectric waveguide, Antenna arrays, Quarter-wavelength pins, Millimeter waveband

1 Introduction

The 5G cellular networks have revolutionized communication by offering enhanced quality of service (QoS) through faster speeds, decreased latency, increased capacities, broader bandwidths, extensive connectivity, improved reliability, and faster response times. As a result, these networks have been deployed across a range of sectors, such as autonomous driving, banking, health care, and education [1–7]. In recent years, there has been a sustained interest in antennas based on dielectric waveguide structures [8–14]. These antennas offer several advantages compared to classical waveguide-slot arrays [15–18].

Dielectric waveguide antennas can achieve higher radiation efficiency compared to classical waveguide-slot arrays [19, 20]. This is because dielectric waveguides reduce losses associated with conductor resistance and radiation leakage [21–23]. They also provide wider bandwidth capabilities compared to classical waveguide-slot arrays [24, 25]. The use of dielectric materials allows for better impedance matching

and broader operating frequency ranges [26–28]. Additionally, the use of dielectric materials allows for miniaturization and integration of the antenna elements, making them suitable for applications where space is limited [29, 30]. Furthermore, dielectric waveguide antennas exhibit low cross-polarization levels compared to waveguide-slot arrays [31–33], which means that the antenna can effectively transmit or receive signals with minimal interference from undesired polarizations [34, 35].

By carefully designing the dielectric structures, the antenna can achieve desired radiation characteristics, such as beam steering and shaping [36–38]. The simplified design and manufacturing process of dielectric waveguide antennas can lead to lower production costs [39–41], which is particularly significant for millimeter-range antennas. The transverse polarization in electromagnetic waves pertains to polarization perpendicular to the waveguide axis. In antenna design, it arises when transverse components of the electromagnetic field near a dielectric rod induce currents, producing a wave polarized transversely to the waveguide axis. Overall, the advantages of dielectric waveguide antennas make them a promising choice for various applications, including wireless communication systems, radar systems, and satellite communication [42, 43].

Therefore, this study aims to conduct a comparison between two types of dielectric waveguide antennas: one with grooves in the dielectric and the other with quarter-wavelength cylindrical pins to distinguish some parameters. The antenna with grooves produces longitudinal polarization [44, 45], with the electric field oriented parallel to the waveguide axis, while the antenna with quarter-wavelength pins has the electric field perpendicular to the waveguide axis [46, 47]. The radiation pattern of the grooved antenna tends to be broadside, with radiation mainly concentrated perpendicular to the waveguide axis [48, 49], while the antenna with quarter-wavelength pins tends to have an end-fire radiation pattern, concentrating the radiation parallel to the waveguide axis [50–52]. Both antennas can achieve wide bandwidth, with the grooved type enhancing impedance matching and reducing reflections, while the quarter-wavelength pins provide higher directivity, resulting in a more focused beam and increased gain [53–55]. The presence of grooves in the dielectric simplifies the fabrication process for antennas, making them cost-effective to manufacture, but the presence of quarter-wavelength pins enables control over beam steering and shaping, allowing for flexibility in directing the antenna's radiation. Also, both types of antennas have their unique strengths and applications. The choice between them depends on specific requirements, such as polarization needs, radiation pattern preferences, bandwidth requirements, and space constraints.

In our previous work, we explored the use of a grooved dielectric waveguide antenna with a periodic system of irregularities, which resulted in the transformation of surface waves into radiating waves [56]. Building upon this foundation, the current study delves into the design of antennas for the extremely high-frequency (EHF) band using dielectric waveguide structures. The focus is on proposing various linear antenna configurations that incorporate metal pins positioned on the side walls of the dielectric groove. One of the key challenges addressed in this study is the issue of cross-polarized radiation in directions near the waveguide axis. To mitigate this, a modified antenna design featuring a closed gutter and a longitudinal slot in the upper wall is introduced. The effectiveness

of these proposed antennas is demonstrated through electrodynamic modeling results obtained from tools such as CST and HFSS.

A substantial number of studies have been conducted to address electrodynamic analysis issues of open waveguide structures [57–59], and provide technical solutions [60, 61]. However, due to the extensive nature of this body of work, it is not feasible to cover all studies within the scope of this article. Therefore, this study focuses on a subset of these works [62–65], that are particularly relevant to the current research. It is important to note that while these antennas offer valuable insights, they also share a common drawback. Specifically, they are equidistant antenna arrays consisting of radiating elements installed at distances equal to the wavelength in the waveguide, which is close to the wavelength in air: $\lambda_{\text{wave}} = \gamma \cdot \lambda_{\text{air}}$, where $\gamma < 1.1 \dots 1.2$. As a result, in directions close to the axial direction, there is an increased level of sidelobes in the antenna radiation pattern, caused by the proximity of secondary maxima determined by a specific condition [63]:

$$\sin \theta_{\text{max}} = m \frac{\lambda_{\text{air}}}{\lambda_{\text{wave}}} \quad (1)$$

The remainder of this paper is organized as follows. Section 2 presents the methodology of antennas for the EHF band using dielectric waveguide structures. The contribution and advantages of the proposed work were involved. Also, a comparison is made between an antenna with grooves in the dielectric and an antenna with metal pins positioned on the side walls of the dielectric groove. Section 3 details the synthesis of LWAs with quarter-wavelength pins and a slot along the waveguide's axis. Section 4 presents the simulation results of the modified transverse polarization antenna. Finally, Section 5 concludes the paper and summarizes the feasibility of the transverse polarization radiation antenna.

2 Methods

In the classical configuration, antennas of this type consist of a dielectric waveguide with a periodic system of irregularities in the form of metallic strips or slots embedded in the dielectric material. The operation of such antennas is explained by transforming the non-radiating surface wave in the homogeneous dielectric structure into a volumetric spatial wave that propagates freely in the surrounding space. Typically, the waveguide dimensions exclude the propagation of any wave types other than the fundamental HE₁₀ mode. The presence of irregularities leads to the generation of polarization in the plane of the antenna axis, while the cross-polarized component is negligible, as depicted in Fig. 1.

The proposed antenna is considered an antenna array with serial excitation. The energy approach is a commonly employed method for the approximate analysis of linear radiating systems designed as a periodic arrangement of identical radiators with a sequential excitation scheme. This study investigates the proposed antenna methodology, integrating a customized energy approach, which provides the characteristics of an almost periodic system radiator. According to the specified approach, a dielectric waveguide with irregularities is represented by an antenna array model with a serial excitation of its elements.

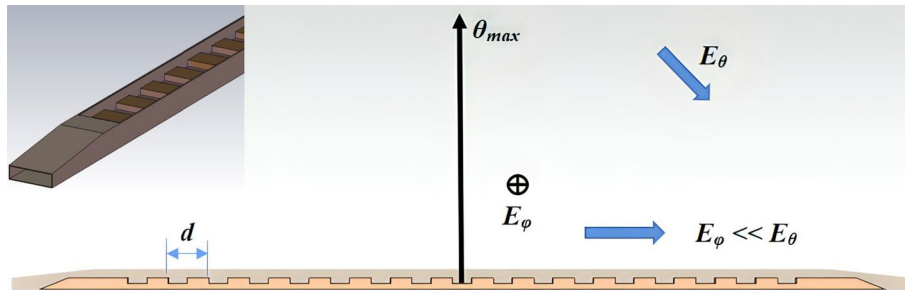


Fig. 1 Radiation formation of the proposed antenna with grooves in the dielectric for polarization in the plane of the antenna axis

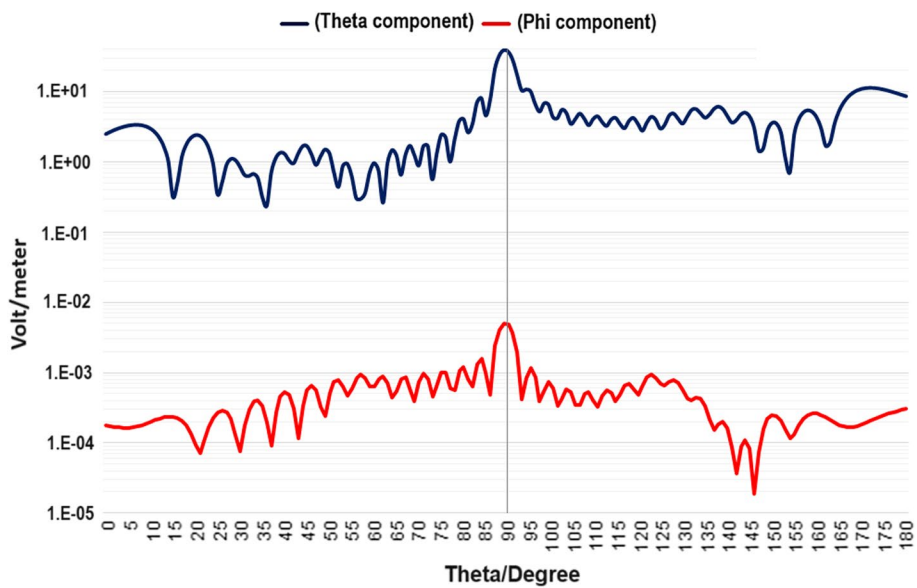


Fig. 2 Numerical CST simulation results of E-field amplitude (Theta and Phi components) in logarithmic scale versus Theta angle at $\varphi = 90^\circ$

As an illustration, the results of modeling an antenna on a waveguide with grooves in the dielectric rod are shown in Figs. 2 and 3. The antenna is composed of 16 elements, and each element is spaced 7.20 mm from the adjacent one. The width and depth of the slots are 3.40 mm and 1.00 mm, respectively, operating at a frequency of 38 GHz, and the dimensions of the metallic waveguide are 7.2×2.0 mm. The analysis results demonstrate that when implementing the transverse radiation mode in these antennas ($d = \lambda_{wave}$), the dominant component is E_θ , i.e., $E_\varphi \ll E_\theta$, indicating polarization in the plane of the antenna, as shown in Figs. 2 and 3.

Figures 2 and 3 represent the antenna radiation pattern by main and cross-polarization indicating polarization in the plane of the antenna, $E_\varphi \ll E_\theta$. The results of modeling an antenna on a waveguide are surrounded by a metal structure with grooves in the dielectric rod opened upper side.

In some cases, there is a need for linear antennas with transverse polarization of the emitted waves. A classical option for such antennas is a waveguide-slot array with

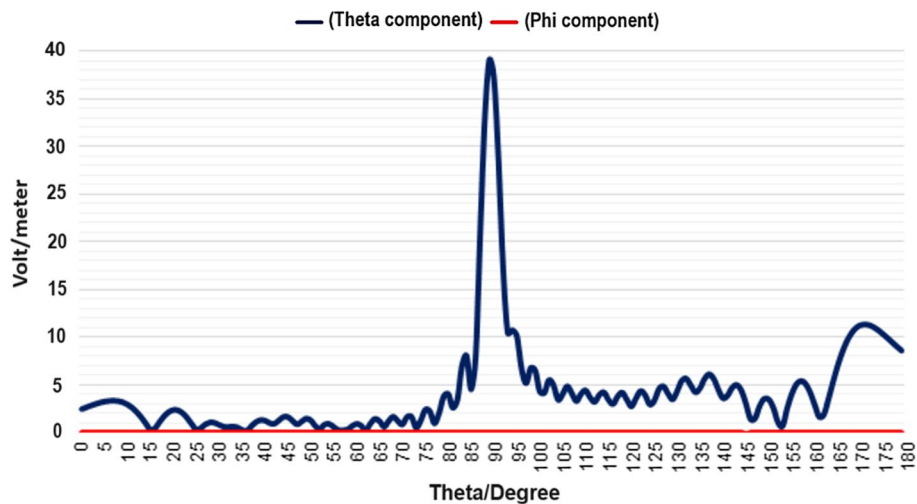


Fig. 3 The CST numerical simulations depict the E-field amplitude (Theta and Phi components) on a linear scale as a function of the Theta angle at $\varphi = 90^\circ$ using a far-field approximation for reference distance = 1 m

longitudinal slots on the side wall of a rectangular waveguide. Implementing such antennas in the millimeter wave range is challenging as it requires even higher manufacturing precision as the frequency increases. In the millimeter wave range, it is preferable to use antennas based on dielectric waveguides. This work aims to explore the feasibility of constructing antennas with transverse polarization, based on a dielectric waveguide structure.

By incorporating a sealed upper boundary within the waveguide and introducing a slot along its central axis, it becomes possible to improve the efficiency of the antenna and reduce the presence of far sidelobes in the antenna's radiation pattern of the main beam in the antenna's pattern, as depicted in Fig. 4.

Figures 5 and 6 illustrate the results obtained by simulating the antenna design on a waveguide that includes grooves in the dielectric rod. The antenna shares identical geometric dimensions but includes an upper slot positioned along the axis of the waveguide. It operates at a frequency of 37 GHz, and the metallic waveguide also has dimensions of 7.2×2.0 mm.

Figures 5 and 6 represent the antenna radiation pattern by main and cross-polarization, also indicating that the dominant component is E_θ . The dielectric waveguide is surrounded by a metal structure with a long longitudinal slot for radiating the electromagnetic field and controlling the losses.

Teflon is used for the dielectric part of the proposed antenna, also known as PTFE, is a material with excellent dielectric properties that make it suitable for use in waveguide antennas. It has a high permittivity, low-loss tangent, and high breakdown voltage. Teflon is used to reduce ohmic losses, increase bandwidth, and enhance impedance match, particularly at millimeter wave and terahertz frequencies. It has specific properties such as $\epsilon_r = 2.1$, $\tan\delta = 0.0002$, a breakdown voltage of 60 kV/mm, a melting point of 327 °C, and a density of 2.2 g/cm³.

According to this observation, the electric field strength (E-field) in an open waveguide is significantly higher than that in a closed waveguide with an upper wall slot. This

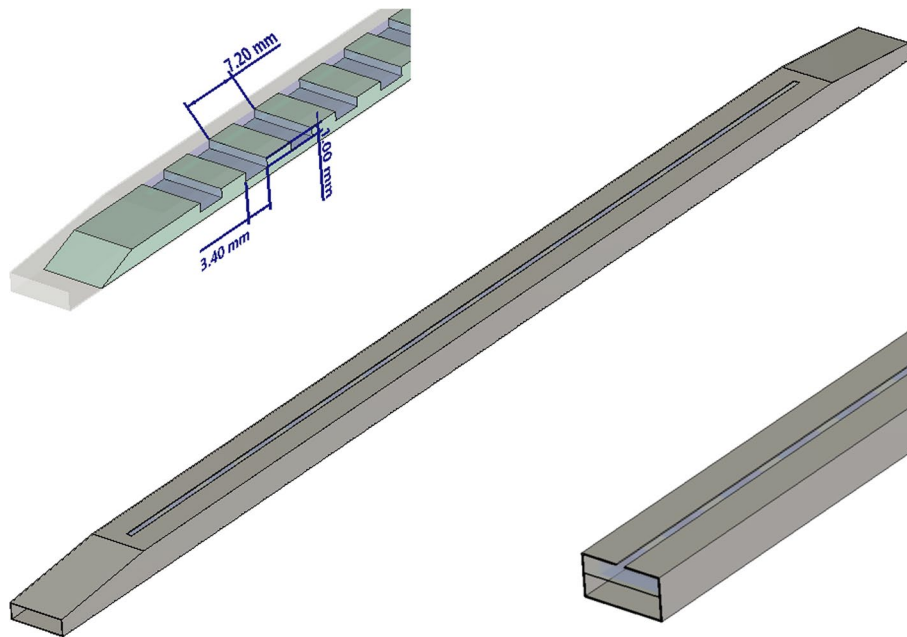


Fig. 4 Antennas with polarization in the plane of the antenna with grooves in the dielectric and a slot along the waveguide’s axis

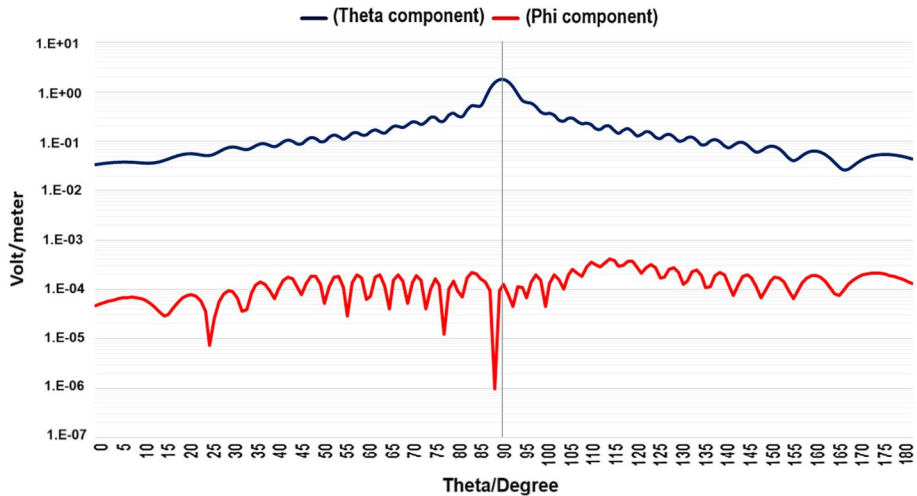


Fig. 5 Numerical CST simulation results of E-field amplitude (Theta and Phi components) in logarithmic scale versus Theta angle at $\varphi = 90^\circ$

contrast arises because the closed upper wall restricts the E_θ component. Nevertheless, this alteration effectively decreases the presence of far sidelobes in the antenna’s radiation pattern.

The difference between the structures designed and simulated lies in the polarization characteristics and modifications made to the antenna design detailed in the following sections. This study compares two types of antennas: one with grooves in the dielectric for longitudinal polarization and another with quarter-wavelength pins for transverse polarization. Additionally, a modified antenna design with a slot along the waveguide’s

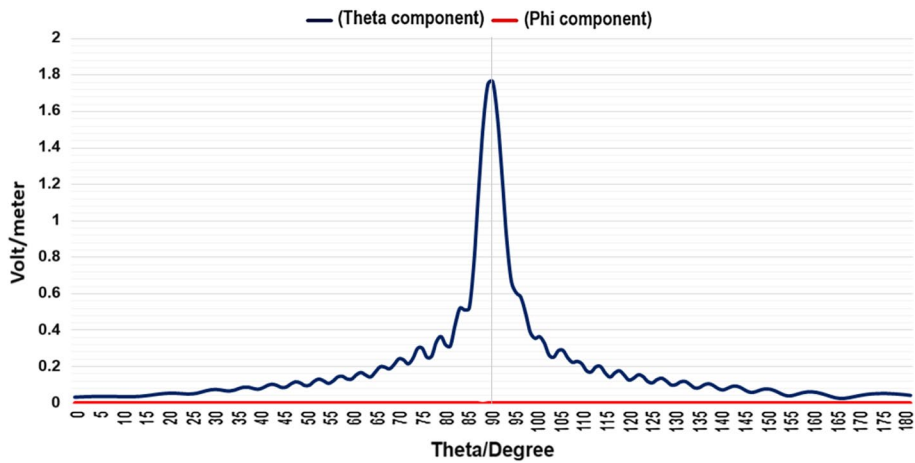


Fig. 6 The CST numerical simulations illustrate the E-field amplitude (Theta and Phi components) in logarithmic scale as a function of the Theta angle at $\varphi = 90^\circ$ using a far-field approximation for reference distance = 1 m

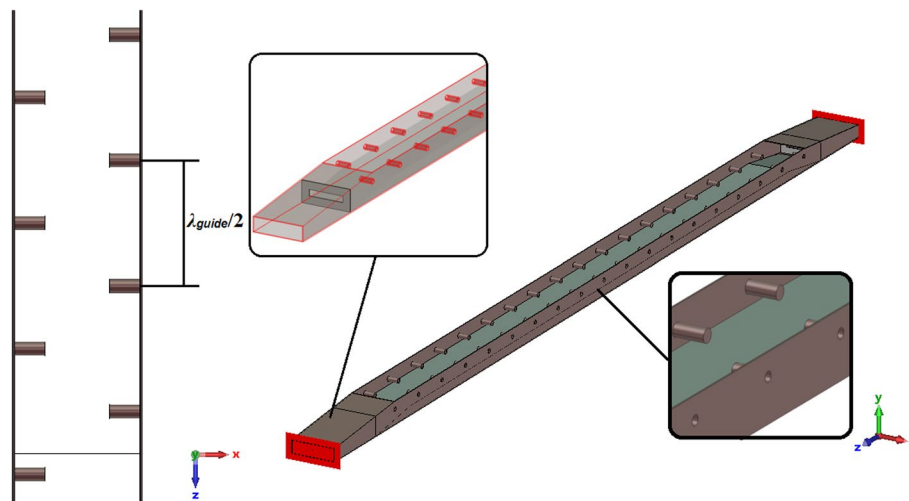


Fig. 7 Antenna with transverse polarization

axis is proposed to reduce cross-polarized radiation and improve the radiation characteristics of the antenna. The simulated structures include antennas with different polarization characteristics and modifications aimed at enhancing the antenna’s performance.

3 An antenna with radiation polarized in a plane perpendicular to the waveguide axis

In [66], an antenna with polarization in a plane perpendicular to the waveguide axis is proposed. The antenna consists of hollow pins arranged in a checkerboard pattern on the side walls of the groove waveguide, as depicted in Fig. 7. The groove dielectric waveguide is designed with electrical dimensions that prevent the propagation of higher-order EH and HE wave types.

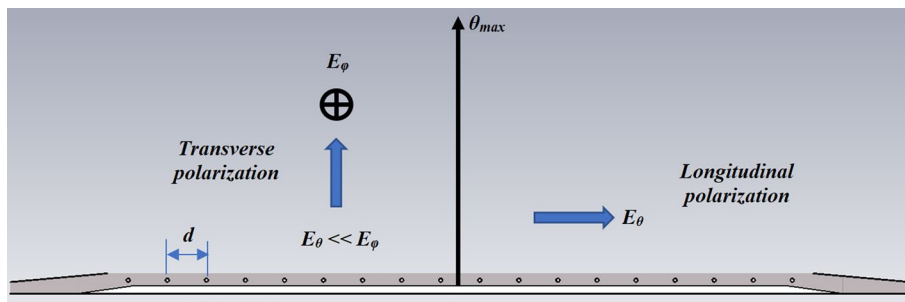


Fig. 8 Antenna radiation: transverse and longitudinal polarization

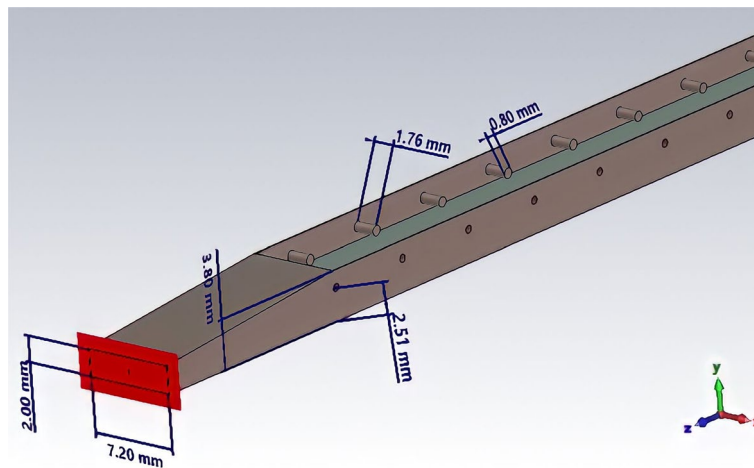


Fig. 9 Antenna with quarter-wavelength pins

The main wave in the vicinity of the dielectric rod exhibits transverse components of the electromagnetic field, inducing currents on their surfaces. As a result, a wave is formed, polarized in the transverse direction to the waveguide axis. If the spacing between adjacent pins is half the wavelength in the waveguide, the radiation characteristics of such an antenna array are like those of a phased array vibrator. However, the presence of irregularities leads to the radiation of the diffracted wave caused by these irregularities. If the waveguide propagates the fundamental mode, its radiation, resulting from the transformation of the surface wave into a volumetric wave, is polarized in the plane of the waveguide. In this case, it can be considered as cross-polarized, as shown in Fig. 8.

To demonstrate the effect of radiation of transverse polarization waves, the calculated radiation patterns are depicted in Fig. 9. The antenna consists of 37 pins, with the dimensions of the waveguide being 7.2×2.0 mm, operating at a frequency of 39 GHz. The length of the pins is 1.76 mm, and the suspension height is 2.51 mm.

The system of opposing pins is excited by a wave in the waveguide that has passed a section of length $\lambda_{\text{guide}}/2$. Therefore, the in-phase superposition of partial fields of transverse polarization occurs in the direction normal to the waveguide. At the same time, the radiation of the “leakage wave” from neighboring sections of the perturbed waveguide is out of phase and mutually canceled. As a result, cross-polarized

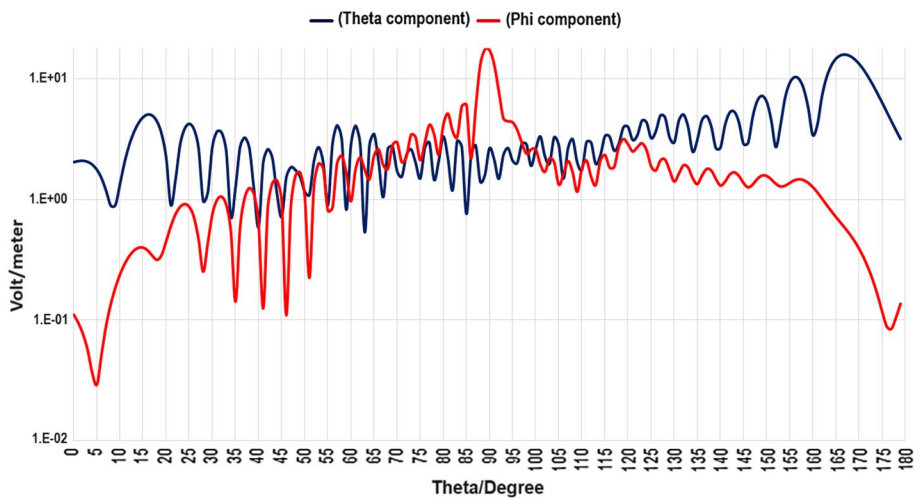


Fig. 10 The numerical simulations conducted in CST demonstrate the E-field amplitude (Theta and Phi components) in logarithmic scale concerning the Theta angle at $\varphi = 90^\circ$, the dominant component is E_φ

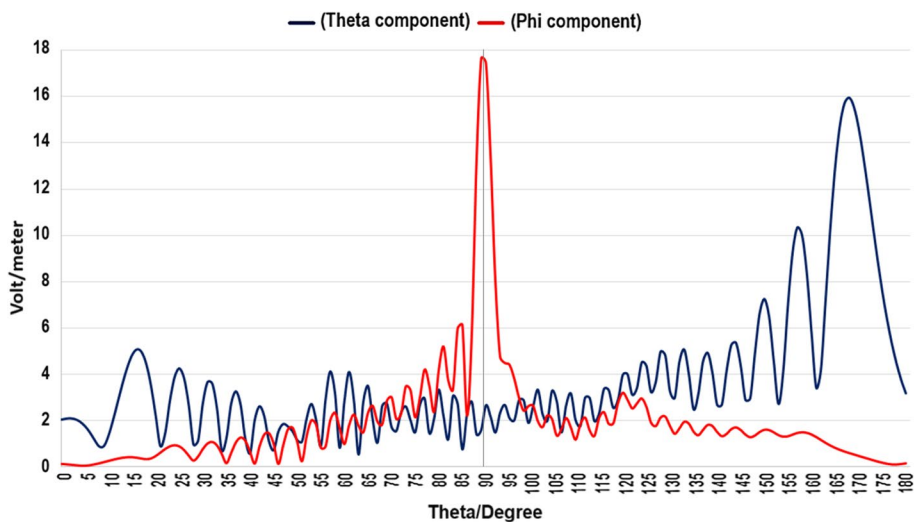


Fig. 11 Numerical CST simulation results of E-field amplitude (Theta and Phi components) in linear scale versus Theta angle at $\varphi = 90^\circ$ using a far-field approximation for reference distance = 1 m

radiation is practically absent in the vicinity of the normal direction. However, in proximity to the axial direction, its intensity can attain a considerable magnitude. The dominant component is E_φ , i.e., $E_\theta \ll E_\varphi$, indicating polarization in the plane of the antenna, shown in Figs. 10 and 11.

Figures 10 and 11 represent the antenna radiation pattern by main and cross-polarization, indicating polarization in the plane of the antenna, $E_\theta \ll E_\varphi$.

4 Simulation and results

4.1 Modified transverse polarization antenna

A drawback of the antenna design [66] is the presence of cross-polarized radiation in directions close to the antenna axis, which is caused by the radiation of the “leakage”

wave. Despite relatively low levels (the level of cross-polarization can be on the order of -10...15 dB), this can lead to a noticeable reduction in the gain in the main polarization.

Let us consider an enlarged-height dielectric groove waveguide enclosed by a conducting material from the top, as depicted in Fig. 12. If the height of the waveguide exceeds the critical radius of the field boundary (on the order of twice the height of the dielectric rod), the presence of the upper “slot” practically does not affect the process of electromagnetic wave propagation. Due to symmetry, the slot cut in the upper lid along the axial line of the waveguide is also not excited by the field of the propagating wave of the main type.

The presence of pins on the side walls of the waveguide disrupts the symmetry of the field in the transverse section, resulting in the emergence of an electric field component perpendicular to the slot in the upper cover. As a result, the mentioned slot radiates into the surrounding space with polarization perpendicular to the waveguide axis. Due to the practical absence of transverse currents in the symmetry plane of the waveguide with a longitudinal slot, the radiation of the wave with a longitudinal component of the electric field, caused by the “leakage” effect of the wave, is significantly less intense. Therefore, there is a reduction in the cross-polarized component of the radiation field in an antenna that exhibits transverse polarization.

Figures 13 and 14 show the antenna radiation pattern in both main and cross-polarization, highlighting that the dominant component is E_φ . The dielectric waveguide is encased in a metallic structure featuring an elongated longitudinal slot for emitting the electromagnetic field.

The inclusion of a sealed upper boundary in the antenna design is motivated by the arrangement of a dielectric rod with two sets of metal conductors placed asymmetrically to the rod’s axis, separated by half the wavelength. The dielectric rod is situated in an enlarged E-plane rectangular waveguide, electrically connected to the E-sector horn around the entire perimeter of the waveguide cross-section. Additionally, a slot

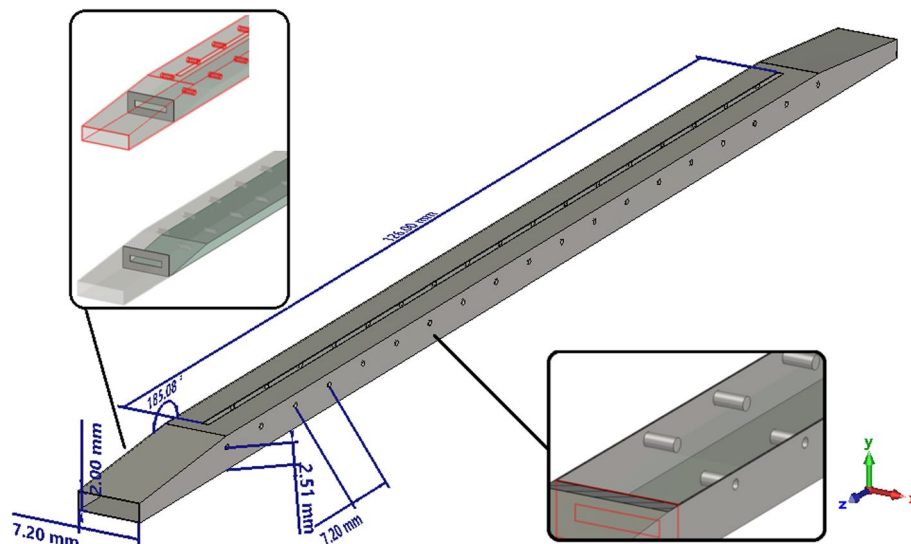


Fig. 12 Antenna with quarter-wavelength pins and a slot along the waveguide’s axis

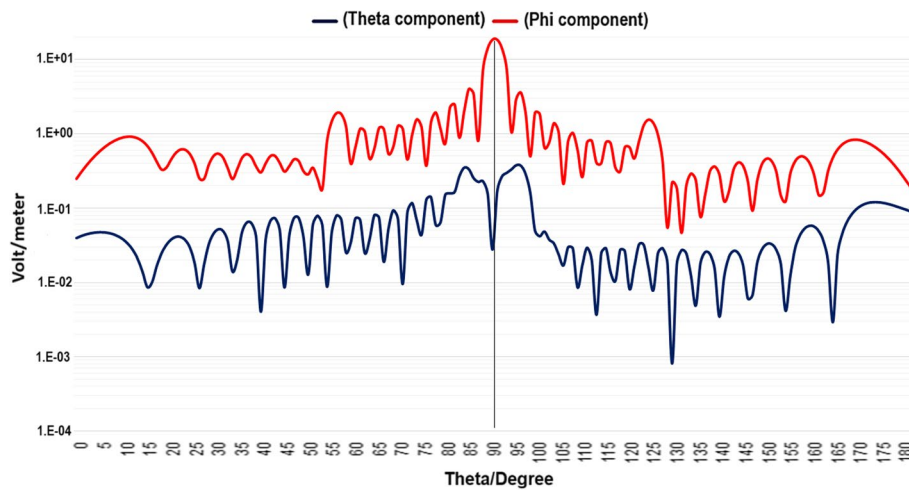


Fig. 13 Numerical CST simulation results of E-field amplitude (Theta and Phi components) in logarithmic scale versus Theta angle at $\varphi = 90^\circ$

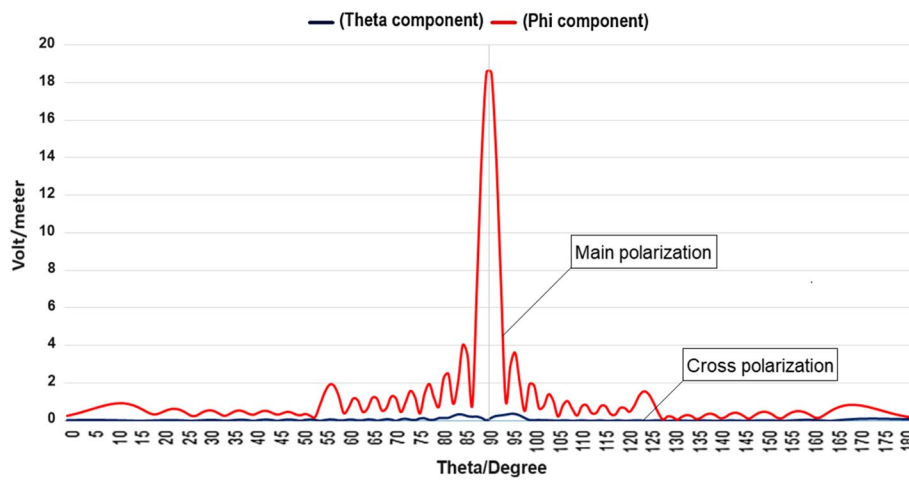


Fig. 14 The CST numerical simulations reveal the E-field amplitude (Theta and Phi components) in a linear scale concerning the Theta angle at $\varphi = 90^\circ$. The simulation employs a far-field approximation, with a reference distance set at 1 m

is cut along the axis of symmetry in the upper wall of the E-sector horn. This design yields enhanced antenna efficiency and a decrease in far sidelobe levels within the antenna pattern [63].

Calculations conducted using electromagnetic modeling in CST Microwave Studio confirm the achievement of the effect of cross-polarized radiation attenuation. The radiation pattern for the main and cross-polarization of the proposed antenna configuration is shown in Figs. 13 and 14. The antenna shares identical configurations with the preceding one, comprising 37 elements arranged in a checkerboard pattern, with a spacing equivalent to half the wavelength in the waveguide. The dielectric rod has dimensions of 7.20 x 1.40 mm, a suspension pin’s height of 2.51 mm, and the dimensions of the waveguide are 7.2 x 2.0 mm. The operating frequency is 39 GHz.

The design provides S_{11} , a radiation pattern and electric field distribution of antenna as shown in Figs. 15, 16, 17, and 18. S_{11} equals -19.58 dB at frequency 39 GHz as shown in Fig. 15. Figures 16 and 17 show that the calculated radiation pattern at frequency $F = 39$ GHz is 19.8 dBi, the width of the radiation pattern is 3.2° , and the side lobe equals -13.3 dB.

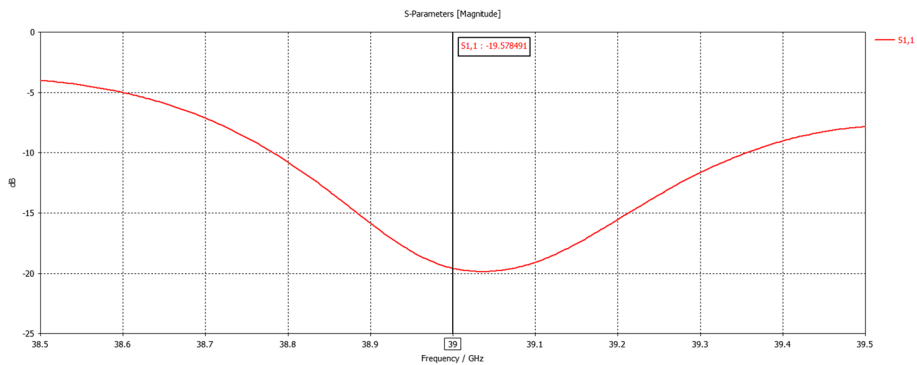


Fig. 15 Simulated reflection coefficient S_{11} at frequency $F = 39$ GHz of the proposed antenna with quarter-wavelength pins and a slot along the waveguide’s axis

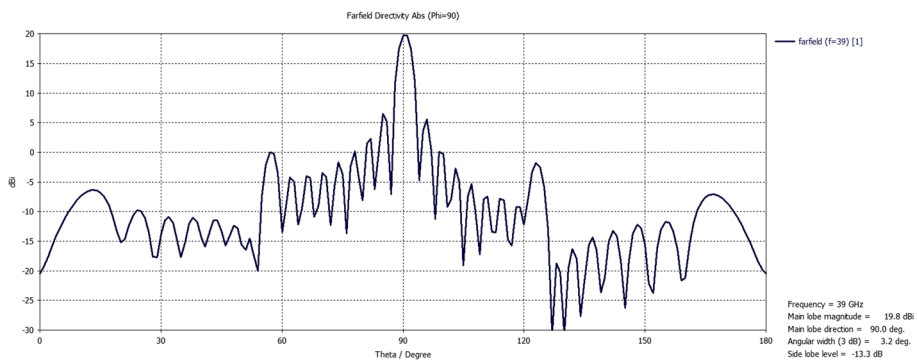


Fig. 16 One-dimensional radiation pattern at frequency $F = 39$ GHz for a proposed antenna with quarter-wavelength pins and a slot along the waveguide’s axis

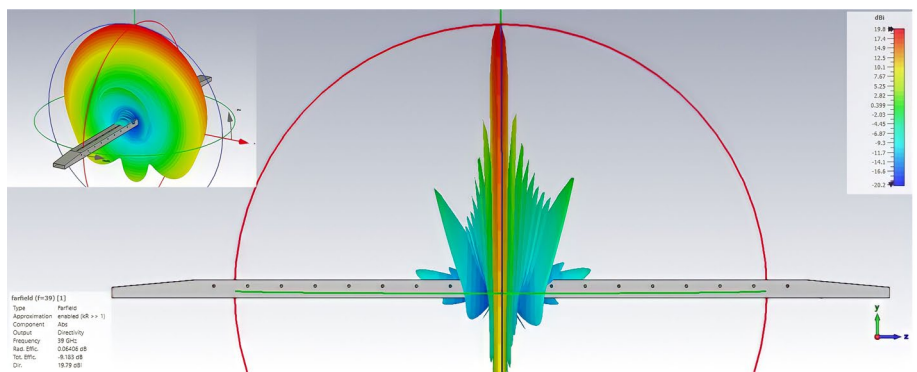


Fig. 17 Three-dimensional radiation pattern at frequency $F = 39$ GHz (RP: 19.8 dBi, width of RP 3.2° , and side lobe: -13.3 dB) for a proposed antenna with quarter-wavelength pins and a slot along the waveguide’s axis

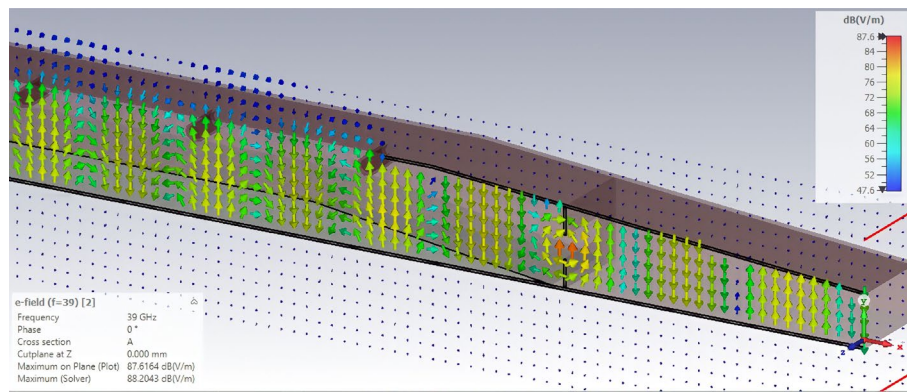


Fig. 18 Three-dimensional electric field distribution of proposed antenna with quarter-wavelength pins and a slot along the waveguide’s axis at 39 GHz

Table 1 The relationship between radiation efficiency and upper slot width

Slot width	VSWR	Γ	η
0.8 mm	1.23	0.1034	0.9893
1.52 mm	1.28	0.1236	0.9847
2.22 mm	1.36	0.1525	0.9768
2.94 mm	1.32	0.1381	0.9809
3.64 mm	1.23	0.1034	0.9893
4.36 mm	1.37	0.1562	0.9756
5.06 mm	1.39	0.1639	0.9731
5.78 mm	1.53	0.2099	0.9560
6.5 mm	1.71	0.2623	0.9311
7.2 mm (fully open)	1.86	0.3019	0.9088

The incorporation of an upper boundary featuring a slot within the waveguide has demonstrated a notable enhancement in the antenna’s efficiency. This improvement arises from the effective reduction of far sidelobes in the radiation pattern of the main beam.

Table 1 provides the correlation between radiation efficiency and the upper slot width in a waveguide employing side-wall-mounted pins at a frequency of 39 GHz. In the computation of antenna efficiency, any losses in the dielectric and metal components of the antenna were disregarded.

A comparison of this work with other arrays in similar frequency bands based on the use of layer slotted waveguides is provided in Table 2. This includes gap waveguides [67], groove gap waveguides [68, 69], and slotted waveguide in groove gap waveguide (GGWG) implemented with glide symmetric holes [70], in conventional rectangular waveguide (RWG) [71], and in SIW [72]. The antenna design with quarter-wavelength pins and a slot along the waveguide’s axis achieves high gain, low sidelobe levels, reduced far sidelobes in the radiation pattern, and improved signal quality, leading to efficient and accurate signal transmission and reception with reduced interference.

Table 2 Performance comparison of the presented waveguide arrays

Works	Freq. (GHz)	Element	Gain	SLL (dB)	Array type
[67]	35	200	31.5	N/A	GWG
[68]	28	N/A	23.68	N/A	GGWG
[69]	28.6	4×9	24.8	−11.5	GGWG
[70]	28	4×4	19.6	−13	GGWG
[71]	25.3	20×16	30.5	−14.7	RWG
[72]	31.5	8×8	18.74	−11.02	SIW
This work	39	18+19	19.8	−13.3	Waveguide antenna with quarter-wavelength pins

5 Conclusion

The feasibility of the transverse polarization radiation antenna has been confirmed through electromagnetic modeling. An identified limitation of this antenna is the notable occurrence of cross-polarized radiation in directions near the antenna axis. To address this drawback, a modified version of the antenna has been proposed. The efficacy of the proposed modifications to antennas with transverse polarization radiation has been validated through electromagnetic modeling.

Abbreviations

GWG	Gap waveguide
GGWG	Groove gap waveguide
SIW	Substrate-integrated waveguide
RGW	Ridge gap waveguide
RWG	Rectangular waveguide
QoS	Quality of service
LWA	Leaky-wave antennas

Acknowledgements

Not applicable.

Author Contributions

Dr. Mohamed N. Shaaban and Prof. Yuri E. Sedelnikov contributed to conceptualization; Dr. Mohamed N. Shaaban and Dr. Aydar R. Nasybullin were involved in formal analysis and funding acquisition; Dr. Mohamed N. Shaaban and Dr. Aydar R. Nasybullin contributed to investigation and writing—original draft, and provided resources and software; Prof. Yuri E. Sedelnikov was involved in methodology; and Dr. Mohamed N. Shaaban and Prof. Yuri E. Sedelnikov contributed to project administration, supervision, and writing—review editing. All authors read and approved the final manuscript.

Funding

Open access funding provided by The Science, Technology & Innovation Funding Authority (STDF) in cooperation with The Egyptian Knowledge Bank (EKB).

Availability of data and materials

Not applicable.

Declarations

Consent for publication

All authors have agreed and given their consent for submission of this paper to the EURASIP Journal of Wireless Communications and Networking.

Competing interest

The authors declare that they have no competing interests.

Received: 11 July 2023 Accepted: 14 March 2024

Published online: 28 March 2024

References

1. B.S. Bismi, S. Azeem, A survey on increasing the capacity of 5g fronthaul systems using ROF. *Opt. Fiber Technol.* **74**, 103078 (2022)
2. S. Senger, P.K. Malik, A comprehensive survey of massive-mimo based on 5g antennas. *Int. J. RF Microwave Comput. Aided Eng.* **32**(12), e23496 (2022)
3. Murtadha Hassan Najji, Ahmed Ghanim Wadday, Mueen Mohsin Abbood, Ahmed Fahem Al-Baghdadi, Bashar Jabbar Hamza, A survey-comprehensive study of 5g architecture. In *AIP Conference Proceedings*, volume 2776. AIP Publishing (2023)
4. R. Singh, A. Mehbodniya, J.L. Webber, G. Pankaj Dadheech, M.S. Pavithra, R.A. Alzaidi, Analysis of network slicing for management of 5g networks using machine learning techniques. *Wirel. Commun. Mobile Comput.* **2022**, 1–10 (2022)
5. H. Babbar, S. Rani, O. Bouachir, M. Aloqaily, From massive IOT toward IOE: evolution of energy efficient autonomous wireless networks. *IEEE Commun. Standards Magazine* **7**(2), 32–39 (2023)
6. M. Pons, E. Valenzuela, B. Rodríguez, J.A. Nolasco-Flores, C. Del-Valle-Soto, Utilization of 5G technologies in IOT applications: current limitations by interference and network optimization difficulties-a review. *Sensors* **23**(8), 3876 (2023)
7. M.S. Abood, H. Wang, D. He, Z. Kang, A. Kawoya, Intelligent network slicing in v2x networks-a comprehensive review. *J. Artif. Intell. Technol.* **3**(2), 75–84 (2023)
8. P. Petroustos, S. Koulouridis. Hybrid glide symmetries and printed periodic surfaces for leakage and mutual reduction on slotted antennas fed by groove gap waveguide. in *2023 17th European Conference on Antennas and Propagation (EuCAP)*, pages 1–5, 2023
9. W. Yong, A. Vosoogh, A. Bagheri, C. Van de Ven, A. Haddadi, A. Alayon Glazunov, An overview of recent development of the gap-waveguide technology for mmwave and sub-thz applications (2023)
10. Y. Li, S. Liao, Q. Xue, W. Che, Coupling analysis of polytetrafluoroethylene dielectric waveguides in the sub-thz band. *Microwave Opt. Technol. Lett.* **65**(10), 2691–2696 (2023)
11. V.V. Klimov, D.V. Guzatov, Perfect invisibility modes in dielectric nanofibers. In *Photonics* **10**, 248 (2023)
12. X. Zhou, Q. Tan, H. Zhang, W. Zhou, X. Huang, High performance chirality-distinguishing beamsplitter based on the dielectric-metal hybrid waveguides. *Opt. Commun.* **527**, 128940 (2023)
13. L. Huang, X. Lei, D.A. Powell, W.J. Padilla, A.E. Miroshnichenko, Resonant leaky modes in all-dielectric metasystems: fundamentals and applications. *Phys. Rep.* **1008**, 1–66 (2023)
14. S. Qi, J. Zhao, W. Wu, Ka-band high-efficiency leaky-wave broadside array antenna based on dielectric image lines. in *IEEE Antennas and Wireless Propagation Letters* (2023)
15. X. Chen, H. Li, X. Liang, X. Zhang, R. Jin, C. Xia, S. Yuezeng, Design of dual-stopband rectangular waveguide slot array antennas. *IEEE Trans. Antennas Propag.* **71**(5), 3905–3915 (2023)
16. S. Farjana, E. Alfonso, P. Lundgren, V. Vassilev, P. Enoksson, A. Uz Zaman. Multilayer dry film photoresist fabrication of a robust > 100 ghz gap waveguide slot array antenna. in *IEEE Access* (2023)
17. J. Gao, T. Li, H. Wang, X. Lei, K. Wang, A compact dual-band dual-linearly polarized waveguide slot array antenna with groove at waveguide bottom. *Int. J. Microwave Wirel. Technol.* **15**(7), 1205–1211 (2023)
18. Q. You, Y. Wang, M. Huang, J. Huang, Z.-W. Zheng, L. Yunlong, Wideband dual-polarized hollow-waveguide slot array antenna. *IEEE Trans. Antennas Propag.* **70**(10), 9326–9336 (2022)
19. Y. Torabi, G. Dadashzadeh, A. Lalbakhsh, H. Oraizi, High-gain and low-profile dielectric-image-line leaky-wave-antenna for wide-angle beam scanning at sub-thz frequencies. *Opt. Laser Technol.* **150**, 107968 (2022)
20. M.C. Sahoo, A. Patani, Slotted rectangular dielectric resonator antenna for the application of satellite communication. *Wireless Pers. Commun.* **130**(2), 837–855 (2023)
21. S. Lavadiya, V. Sorathiya, K. Dave, S.V. Kumari, Antennas for thz communication: Fundamentals, design structures, and current trends. In *Terahertz Devices, Circuits and Systems: Materials, Methods and Applications*, pages 183–203. Springer (2022)
22. C. Tong, Pcb materials and design requirements for 5g systems. in *Advanced Materials and Components for 5G and Beyond*, pages 77–108. Springer (2022)
23. I. Peter, S. S. Singhwal, 5g antenna materials and ensuing challenges. In *Printed Antennas for 5G Networks*, pages 311–335. Springer (2022)
24. S. Mohanty, B. Mohapatra, The effect of finite ground plane on wideband slim rectangular dielectric resonator antenna. in *VLSI, Microwave and Wireless Technologies: Select Proceedings of ICVMMT 2021*, pages 791–799. Springer (2022)
25. X. Guofu, M. Skorobogatiy, Wired THz communications. *J. Infrared Millimeter Terahertz Waves* **43**(9–10), 728–778 (2022)
26. R.S. Nishtha, G.V. Yaduvanshi, Isolation control for implementing the single dielectric resonator based tunable thz mimo antenna and filter. *Opt. Quant. Electron.* **55**(4), 357 (2023)
27. Yu. Yuxuan Luo, F. Jiawei, Y. Cheng, H.L. Chen, A compact microwave bandpass filter based on spoof surface plasmon polariton and substrate integrated plasmonic waveguide structures. *Appl. Phys. A* **128**(2), 97 (2022)

28. Y. Li, S. Liao, Q. Xue, W. Che, Transmission characteristics of flexible low-loss solid circular polymer dielectric waveguides for sub-thz applications. *J. Infrared Millimeter Terahertz Waves* **44**(1–2), 110–133 (2023)
29. R. Adhikari, Z. Sbeah, R. Gupta, D. Chauhan, J.-M. Nunzi, R.P. Dwivedi, Compact and sensitive h-shaped metal-dielectric-metal waveguide plasmonic sensor. *Plasmonics* **17**(4), 1593–1606 (2022)
30. S. Dwivedi, Design and analysis of metamaterial waveguide antenna for broadband applications. in *ICT Analysis and Applications: Proceedings of ICT4SD 2022*, pages 417–423. Springer (2022)
31. M. Agrawal, K. Saraswat, T. Kumar, Wideband substrate integrated waveguide based dual-polarized antenna for satellite applications in ku-band. in *Evolution in Signal Processing and Telecommunication Networks: Proceedings of Sixth International Conference on Microelectronics, Electromagnetics and Telecommunications (ICMEET 2021), Volume 2*, pages 115–123. Springer (2022)
32. R. Samson Daniel, Dual-band siw cavity backed antenna loaded with CSRR metamaterial. *Microsyst. Technol.* **29**(3), 337–345 (2023)
33. G.S. Karthikeya, M. Idrees Magray, C. Zebiri, J.H. Tarng, S.K. Koul, Implementational aspects of various feeding techniques for mmwave 5g antennas. *Arab. J. Sci. Eng.* **47**(11), 14731–14744 (2022)
34. G. Xue, L. Lin, Q. Zhai, C. Zeng, X. Wang, X. Li, Development of dielectric-film-based polarization modulation scheme for patterning highly uniform 2d array structures with periodic tunability. *Opt. Lasers Eng.* **167**, 107627 (2023)
35. T. Nahar, S. Rawat, Efficiency enhancement techniques of microwave and millimeter-wave antennas for 5g communication: A survey. *Trans. Emerg. Telecommun. Technol.* **33**(9), e4530 (2022)
36. Q. Ali, W. Shahzad, I. Ahmad, S. Safiq, X. Bin, S.M. Abbas, H. Sun, Recent developments and challenges on beam steering characteristics of reconfigurable transmitarray antennas. *Electronics* **11**(4), 587 (2022)
37. R.V. Gatti, SwanTM-cad tool for the design and analysis of large beam steering slotted waveguide arrays. in *2022 IEEE International Symposium on Phased Array Systems & Technology (PAST)*, pages 01–07. IEEE (2022)
38. A. Pattanayak, A. Hati, S. P. Duttagupta, Beam steering of antenna array using phase gradient metasurface. in *Handbook of Metamaterial-Derived Frequency Selective Surfaces*, pages 395–425. Springer (2023)
39. M. Bauer, C. Matheis, A. Mashkin, S. Krane, Friedhelm Pohlmann, Fabian Friederich, Terahertz non-destructive testing of the mica insulation of power generator bars in fmcw measurements with a dielectric waveguide antenna. in *2021 51st European Microwave Conference (EuMC)*, pages 805–808. IEEE (2022)
40. Y. Li, S. Liao, Q. Xue, W. Che, Transmission characteristics of flexible low-loss solid circular polymer dielectric waveguides for sub-thz applications. *J. Infrared Millimeter Terahertz Waves* **44**(1–2), 110–133 (2023)
41. A. Simonovic, E. Rohwer, T. Stander, Sla-printed k-band waveguide components using tollens reaction silver plating. *IEEE Trans. Components Packag. Manuf. Technol.* **13**(2), 230–239 (2023)
42. S. Kavitha, K. Sairam, A. Singh, Y-shaped plasmonic waveguide splitter coupled with nano-antenna for optical wireless communication. *Arab. J. Sci. Eng.* **48**(11), 15015–15027 (2023)
43. Ildiko Peter, Sumer Singh Singhwai, 5g antenna materials and ensuing challenges. In *Printed Antennas for 5G Networks*, pages 311–335. Springer (2022)
44. W. Xiaoer, J. Xiao, Full-vectorial meshfree method with an efficient iteration scheme for full anisotropic optical waveguides. *Opt. Quant. Electron.* **54**(5), 299 (2022)
45. A. Degtyarev, M. Dubinin, O. Gurin, V. Maslov, K. Mutean, V. Ryabykh, V. Senyuta, O. Svystunov, Control over higher-order transverse modes in a waveguide-based quasi-optical resonator. *Radio Phys. Radio Astron.* **27**(2), 129 (2022)
46. J.-Y. Chung, G. Yih, Low-profile vhf antenna based on quarter-mode substrate-integrated waveguide structure. *Appl. Sci.* **12**(18), 8973 (2022)
47. Anish Ramkishan Mishra, Microstrip-to-waveguide transition for 140 ghz using gap waveguide technology (2022)
48. L. Zou, Z. Li, L. Liu, J. Wang, A design method for a leaky-wave system with uniform field coverage and broadside radiation for a vacuum-tube ultra-high-speed train. *IEEE Trans. Antennas Propag.* **70**(10), 9936–9941 (2022)
49. A. Aziz, A. Aziz, A novel plasmonic waveguide for the dual-band transmission of spoof surface plasmon polaritons. *Eur. Phys. J. Plus* **137**(5), 605 (2022)
50. M. Li, S.-K. Li, M.-C. Tang, L. Zhu, A compact, single-layer, index-modulated microstrip antenna with stable customized tilted beam over a wide bandwidth. *IEEE Trans. Antennas Propag.* **70**(12), 11465–11474 (2022)
51. S.K. Ibrahim, M.J. Singh, S.S. Al-Bawri, H.H. Ibrahim, M.T. Islam, M.S. Islam, A. Alzamil, W.M. Abdulkawi, Design, challenges and developments for 5g massive mimo antenna systems at sub 6-ghz band: A review. *Nanomaterials* **13**(3), 520 (2023)
52. A. Pickering, *Multi-antenna fixed position system for lesion detection within phantoms*. PhD thesis, London South Bank University (2022)
53. W. Kang, T.-H. Lim, Y. Kim, S. An, J.-H. Joo, G. Byun, Design of a compact indirect slot-fed wideband patch array with an air siw cavity for a high directivity in missile seeker applications. *Appl. Sci.* **12**(19), 9569 (2022)
54. W. Yuan, J.F. Chen, C. Zhang, W.X. Tang, L. Wang, Q. Cheng, T.J. Cui, Glide-symmetric lens antenna in gap waveguide technology. *IEEE Trans. Antennas Propag.* **68**(4), 2612–2620 (2019)
55. Y. Torabi, G. Dadashzadeh, M. Hadeie, H. Oraizi, A. Lalbakhsh, A wide-angle scanning sub-terahertz leaky-wave antenna based on a multilayer dielectric image waveguide. *Electronics* **10**(17), 2172 (2021)
56. M.N. Shaaban, M.H.E. Ali, M.S. Yasseen, A.R. Nasybullin, Y.E. Sedelnikov, A promising ka band leaky-wave antenna based on a periodic structure of non-identical irregularities. *EURASIP J. Wirel. Commun. Netw.* **2022**(1), 1–16 (2022)
57. V. Gridnev, Analysis of the characteristics of slot radiators on siw waveguides by the galerkin method. in *2022 IEEE 8th All-Russian Microwave Conference (RMC)*, pages 167–169. IEEE (2022)
58. Y. Shestopalov, Y. Smirnov, E. Smolkin, Open waveguides of arbitrary cross section. in *Optical Waveguide Theory: Mathematical Models, Spectral Theory and Numerical Analysis*, pages 221–258. Springer (2022)
59. I. Islamov, E. Humbataliyev, General approaches to solving problems of analysis and synthesis of directional properties of antenna arrays. *Adv. Electromag.* **11**(4), 22–33 (2022)

60. E. Z. Hunbatallyev, Mathematical modeling of an antenna device based on a t-shaped waveguide of the microwave range. in *The International Conference on Artificial Intelligence and Applied Mathematics in Engineering*, pages 16–29. Springer (2022)
61. M. E. Rao, T. Maetz, J. Moll, Numerical analysis of dispersion compensation for guided electromagnetic waves in rectangular microwave waveguides. in *2022 16th European Conference on Antennas and Propagation (EuCAP)*, pages 1–5. IEEE (2022)
62. P. Lampariello, F. Frezza, A. Galli, P. Baccarelli, P. Burghignoli, G. Lovat, S. Paulotto, G. Valerio, D.R. Jackson, Advances in leaky-wave periodic structures after oliner's pioneering research. in *2014 44th European Microwave Conference*, pages 433–436. IEEE (2014)
63. Y. Evgenevich Sedelnikov, M. N. Shaaban, A. Yurevna Myshkina, Millimeter wave antenna, Patent RU2694156C1 (2019)
64. D.R. Jackson, A.A. Oliner, Leaky-wave antennas, [in modern antenna handbook, c. balanis, ed (2008)
65. D. Hang, Z. Li, J. Wang, Broadband fixed-beam leaky-wave antenna with consistent and high gain based on ridge gap waveguide. *IEEE Antennas Wirel. Propag. Lett.* **21**(9), 1925–1929 (2022)
66. Yuri Evgenevich Sedelnikov, Vladimir Vasilevich Kosorukov, Printed antenna for millimeter wave, Patent SU1513546A1 (1989)
67. L. Kong, C. Jin, H. Han, J. Chen, J. Li, J. Liu, A right-handed circularly polarized array antenna based on gap waveguide technology at 35 ghz. *Microw. Opt. Technol. Lett.* **63**(7), 1955–1959 (2021)
68. N. Memeletzoglou, E. Rajo-Iglesias, Array of stacked leaky-wave antennas in groove gap waveguide technology. *Sci. Rep.* **11**(1), 2260 (2021)
69. Q. Liao, E. Rajo-Iglesias, O. Quevedo-Teruel, ka-band fully metallic te 40 slot array antenna with glide-symmetric gap waveguide technology. *IEEE Trans. Antennas Propag.* **67**(10), 6410–6418 (2019)
70. S. Park, Y. Tsunemitsu, J. Hirokawa, M. Ando, Center feed single layer slotted waveguide array. *IEEE Trans. Antennas Propag.* **54**(5), 1474–1480 (2006)
71. B. Liu, W. Hong, Z. Kuai, X. Yin, G. Luo, J. Chen, H. Tang, W. Ke, Substrate integrated waveguide (siw) monopulse slot antenna array. *IEEE Trans. Antennas Propag.* **57**(1), 275–279 (2009)
72. L.F. Herrán, A.A. Brazalez, E. Rajo-Iglesias, Ka-band planar slotted waveguide array based on groove gap waveguide technology with a glide-symmetric holey metasurface. *Sci. Rep.* **11**(1), 8697 (2021)

Publisher's Note

Springer Nature remains neutral with regard to jurisdictional claims in published maps and institutional affiliations.